

A Method for Overcoming Plasma Protein Inhibition of Tyrosine Kinase Inhibitors



David J. Young^{1,2}, Bao Nguyen¹, Li Li¹, Tomoyasu Higashimoto^{1,3}, Mark J. Levis¹, Jun O. Liu^{1,4}, and Donald Small^{1,2}



ABSTRACT

FMS-like tyrosine kinase 3 (*FLT3*) is the most frequently mutated gene in acute myeloid leukemia and a target for tyrosine kinase inhibitors (TKI). *FLT3* TKIs have yielded limited improvements to clinical outcomes. One reason for this is TKI inhibition by endogenous factors. We characterized plasma protein binding of *FLT3* TKI, specifically staurosporine derivatives (STS-TKI) by alpha-1-acid glycoprotein (AGP), simulating its effects upon drug efficacy. Human AGP inhibits the antiproliferative activity of STS-TKI in *FLT3*/ITD-dependent cells, with IC_{50} shifts higher than clinically achievable. This is not seen with nonhuman plasma. Mifepristone cotreatment, with its higher AGP affinity, improves TKI activity despite AGP, yielding IC_{50} s predicted to be clinically effective. In a mouse model of AGP drug inhibition, mifepristone restores midostaurin activity. This suggests combinatorial methods for overcoming plasma protein inhibition of existing TKIs for leukemia as well as providing a platform for investigating the drug-protein interaction space for developing more potent small-molecule agents.

SIGNIFICANCE: Our data provide a mechanism for the failure of some previous TKI clinical trials. The ability of mifepristone to disinhibit TKIs suggests an approach by which the combination of TKIs with already approved and well-tolerated drugs may restore TKI activity.

INTRODUCTION

FMS-like tyrosine kinase 3 (*FLT3*) is the most frequently mutated gene in acute myeloid leukemia (AML). Approximately one third of adult AML cases and a lower fraction of pediatric AML cases express a *FLT3* mutation (1–3). Wild-type *FLT3* is expressed within early progenitor populations and may also be expressed at a lower level within the hematopoietic stem cell (HSC) compartment. It continues to be expressed during differentiation, decreasing with terminal differentiation, although it does continue through dendritic cell development (4, 5). In disease, *FLT3* mutations lead to constitutive kinase activity, activating multiple signaling pathways including *STAT5*, *AKT*, and *MAPK/ERK* (6, 7). These, in turn, lead to the downstream effects that are the hallmarks of *FLT3*-mutant AML: differentiation blockade, inhibition of apoptosis, and a proliferative advantage.

FLT3 mutations occur in cooperation with mutations in many other genes, most frequently *DNMT3A* and *NPM1*,

and are often the last step leading to transformation to AML (2). The most common mutation is the internal tandem duplication (ITD), an in-frame duplication of a small sequence of variable length within the *FLT3* juxtamembrane domain. This leads to loss of autoregulation and subsequent constitutive *FLT3*/ITD activity. As a high-risk feature, it is associated with increased rates of refractory disease and relapse, and decreased overall survival. In studies, patients with *FLT3*/ITD AML have a 15% to 25% event-free survival in response to standard AML chemotherapy protocols compared with 40% to 60% in patients without (3). As a result, *FLT3*-mutated AML has not benefited from many of the advances seen in outcomes for other leukemias. The addition of bone marrow transplant with its short- and long-term toxicities is necessary to improve outcome. Yet, in contrast to their chemoresistance, AML blasts with *FLT3* mutations are preferentially sensitive to tyrosine kinase inhibitors (TKI) against *FLT3*, making *FLT3* an attractive target for drug development (8).

Despite the promise of *FLT3*-directed therapy, *FLT3* TKI clinical trials have had limited success. Although several *FLT3* TKIs have been approved for clinical use, it is clear that more effective targeting is needed. Multiple factors contributed to these outcomes: *FLT3* resistance mutations, bone marrow stromal-derived survival factors, overexpression of *FLT3* ligand, and activation of alternative “bypass” pathways. The study of these has led to *FLT3* TKIs with ever-increasing efficacy. However, the role of patient-specific factors in modulating treatment efficacy remains relatively unexplored in the context of *FLT3* AML research.

Prior *in vitro* and clinical trial data indicate that the lack of *FLT3*-specific clinical impact by TKI therapy may be due, in part, to inadequate activity against *FLT3* due to inhibition of these agents by patient-specific factors such as plasma protein binding, stromal protection, and altered pharmacokinetics. Indeed, we hypothesize that suppression of *FLT3* TKI-mediated inhibition through plasma protein binding is a leading cause of limited clinical impact. Thus, we have

¹Department of Oncology, Johns Hopkins University School of Medicine, Baltimore, Maryland. ²Department of Pediatrics, Johns Hopkins University School of Medicine, Baltimore, Maryland. ³Department of Human Genetics, Johns Hopkins University School of Medicine, Baltimore, Maryland. ⁴Department of Pharmacology and Molecular Sciences, Johns Hopkins University School of Medicine, Baltimore, Maryland.

Note: Supplementary data for this article are available at Blood Cancer Discovery Online (<https://bloodcancerdiscov.aacrjournals.org/>).

Current address for D.J. Young: National Heart, Lung, and Blood Institute, National Institutes of Health, Bethesda, Maryland.

Corresponding Author: Donald Small, Sidney Kimmel Comprehensive Cancer Center at Johns Hopkins, CRB1 Room 251, 1650 Orleans Street, Baltimore, MD 21231. Phone: 410-614-0994; Fax: 410-955-8897; E-mail: donsmall@jhmi.edu

Blood Cancer Discov 2021;2:532–47

doi: 10.1158/2643-3230.BCD-20-0119

This open access article is distributed under the Creative Commons Attribution-NonCommercial-NoDerivatives License 4.0 International (CC BY-NC-ND).

©2021 The Authors; Published by the American Association for Cancer Research

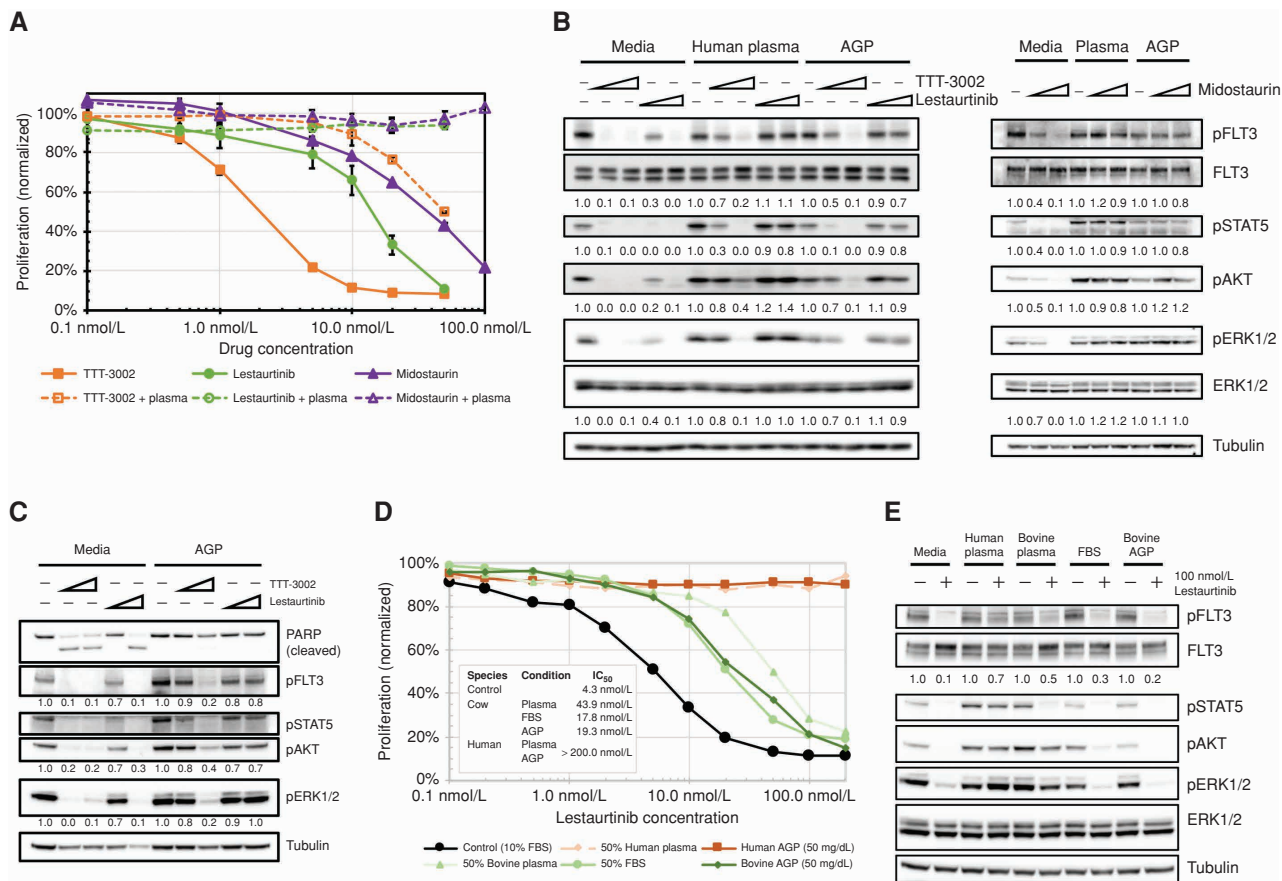


Figure 1. FLT3 inhibitors are differentially inhibited by human plasma and AGP. Coincubation with human plasma or human AGP inhibits FLT3 TKI activity. **A**, Proliferation of MOLM-14 cells after 48 hours of TKI exposure in the presence or absence of 50% human plasma was assessed by colorimetric methods (MTT). **B**, MOLM-14 cells were exposed to low (10 nmol/L) or high (100 nmol/L) concentrations of TKI as well as media (10% FBS), 50% human plasma, or human AGP and analyzed by phospho-Western blotting for FLT3 phosphorylation and downstream signaling. **C**, Western blot analysis for cleaved PARP after 24 hours of TKI exposure under standard culture conditions (10% FBS) or in the presence of either 100% human plasma or purified human AGP. Proliferation (**D**) and Western blot analysis (**E**) experiments were repeated in the presence of 50% FBS, bovine plasma, or purified bovine AGP and compared with comparable results with the corresponding human fractions.

undertaken a study to determine the impact of plasma protein binding on FLT3 TKI activity, focusing on the staurosporine family of which the recently approved drug midostaurin is a member. Furthermore, we report here a method for overcoming plasma protein inhibition to restore the promise of molecularly targeted therapy in FLT3-mutated AML as well as for other TKIs whose activity is diminished by protein binding.

RESULTS

Human Plasma and Plasma Proteins Reduce TKI Efficacy

In the original plasma inhibitory assay (PIA), FLT3/ITD-expressing cells are coincubated with plasma samples from patients receiving a FLT3 TKI, and the extent of FLT3 inhibitory activity present in their plasma is measured by Western blotting analysis of FLT3 autophosphorylation (9). This is compared with total plasma drug levels to determine the relative efficacy of a drug *in vivo* compared with

its activity *in vitro* and thus impute the effects of host factors on drug efficacy beyond simple metabolism. To model these effects in the preclinical setting, we modified the PIA. Whereas the PIA was designed to assess *in vivo* drug activity with regard to a specific target (e.g., inhibition of FLT3 autophosphorylation by TKI), the modified PIA is similarly cell based but measures the clinically relevant biological endpoints of cytotoxicity and proliferation inhibition. In the modified assay, FLT3/ITD cell lines are cultured in the presence of human plasma or purified human plasma proteins and treated with a range of concentrations of the drug of interest. The IC₅₀ measured using the colorimetric MTT method is compared with treatment under typical *in vitro* culture conditions of 10% FBS (Fig. 1A). Like the original PIA, Western blot analysis can be performed on cells treated in this manner to study specific pathways of interest (Fig. 1B). Thus, it is possible to simulate the *in vivo* effect of plasma proteins upon drug activity, allowing one to investigate the effect of endogenous proteins in their native state upon drug dose–response relationships in a controlled

manner without the confounding variables of patient-specific drug bioavailability and metabolism. Utilizing the general endpoint of cytotoxicity, the modified PIA is readily adaptable to other disease types and agents where plasma protein binding has been implicated in affecting therapeutic efficacy.

We treated MOLM-14 cells (FLT3/ITD heterozygous, KMT2A-rearranged myeloid leukemia cell line) for 48 hours with midostaurin, lestaurtinib, or TTT-3002 (a novel FLT3 TKI) across a range of physiologically relevant concentrations in the presence of either 50% human plasma from healthy donors or standard 10% FBS culture conditions (Fig. 1A; refs. 10, 11). For all three TKIs, the addition of human plasma significantly increased the IC_{50} of each drug, and for midostaurin and lestaurtinib, IC_{50} s were no longer reached in the range of the conditions tested.

To demonstrate that this effect is through reduced FLT3 inhibition, we treated MOLM-14 cells with each TKI at concentrations greater than the IC_{50} for inhibition of FLT3 autophosphorylation (10 nmol/L and 100 nmol/L) and assessed FLT3 autophosphorylation and downstream signaling in the presence or absence of human plasma (Fig. 1B). For TTT-3002, the presence of human plasma leads to a significant decrease in inhibition of FLT3 phosphorylation, and decreased downstream inhibition of phosphorylation/activation of STAT5, AKT1, and ERK1/2. Although this effect was overcome by increasing the concentration of TTT-3002, for midostaurin and lestaurtinib, there was no appreciable FLT3 TKI activity in the presence of plasma even with a 10-fold increase in drug. Previous work and clinical trials with FLT3 TKIs have suggested that alpha-1-acid glycoprotein (AGP), an acute-phase acid glycoprotein responsible for scavenging basic drugs and steroids, plays a role in binding FLT3 TKIs (11–17). We repeated these experiments in the presence of physiologically equivalent concentrations of purified AGP (1 mg/mL) instead of whole human plasma, and comparable inhibition of anti-FLT3 activity was again observed (Fig. 1B).

We repeated the modified PIA, assaying for apoptosis after 24 hours, and found that the presence of human plasma abrogates TKI-induced apoptosis (Supplementary Fig. S1A) and associated PARP cleavage (Fig. 1C). Again, the use of physiologic concentrations of human AGP in place of whole plasma is sufficient to reproduce this effect. These results were also seen in the TKI-mediated effects on cell-cycle analysis (Supplementary Fig. S1B). The addition of human AGP alone does not affect FLT3 signaling, baseline apoptosis, or cell-cycle distribution. These data indicate that human AGP plays a significant role in the observed plasma inhibition of TKI activity, presumably sequestering the drugs away from their cellular target. Furthermore, when these experiments are repeated using bovine plasma or bovine AGP, there is little effect on the activity of FLT3 TKIs (Fig. 1D and E). These results, along with the lower expression of AGP in mice and cattle, likely explain why these effects are not observed in pre-clinical *in vitro* and *in vivo* murine studies (18–20).

FLT3 TKIs Are Differentially Affected by Human Plasma and Purified Human Plasma Proteins

We tested a panel of FLT3 TKIs for activity in the modified PIA. All TKIs tested demonstrate increases in IC_{50} in

the presence of 50% human plasma (Fig. 2A). These range from minimal (9-fold) inhibition for TTT-3002 to moderate inhibition (37-fold) for quizartinib to greater than 100-fold inhibition for lestaurtinib, midostaurin, and sorafenib. When tested using purified human AGP at physiologic concentrations (1 mg/mL), quizartinib and sorafenib activity were not significantly inhibited, whereas TTT-3002 demonstrated comparable inhibition to that observed with human plasma (Fig. 2B). Complete inhibition of lestaurtinib and midostaurin activities was observed, even at subphysiologic concentrations. Examination of structures show that the TKIs affected significantly by AGP (lestaurtinib, midostaurin, TTT-3002) are all derivatives of staurosporine, in contrast to those unaffected by AGP (Fig. 2C). In comparison, gilteritinib, the FDA-approved non-staurosporine TKI, is minimally affected by the presence of plasma proteins (Supplementary Fig. S1C).

Plasma AGP Concentration Is the Primary Determinant of Plasma Protein Inhibition of Staurosporine-Derived TKIs

To characterize the impact of human plasma on the staurosporine-derived TKIs, we examined the relationship between fold change in the IC_{50} of TTT-3002 and AGP concentrations. When the modified PIA was performed for TTT-3002 using purified human AGP across a range of concentrations, a relationship was seen between AGP concentration and the associated TTT-3002 dose–response curves (Fig. 3A). Measuring IC_{50} at each AGP concentration and comparing it to that observed under standard culture conditions (IC_{50} fold change), a direct linear relationship was noted between IC_{50} fold change and AGP concentration (Fig. 3B). A similar relationship was noted for lestaurtinib, wherein appreciable activity is seen only at AGP concentrations less than one tenth of physiologic human levels (Supplementary Fig. S2).

As these results suggest that the major determinant of plasma inhibition of staurosporine TKIs is AGP, we studied the relationship of plasma AGP concentration to plasma inhibition. Plasma samples from 19 human donors were collected, AGP concentration was measured (124 ± 66 mg/dL), and TTT-3002 inhibition by the plasma was tested using the modified PIA. There is a linear correlation between plasma AGP concentration in the samples and the resulting IC_{50} fold change (Fig. 3C, solid line), which correlates closely to the results observed using purified AGP (Fig. 3C, dashed line). Furthermore, univariate (R^2) and multivariate analyses (P) of total protein concentration ($R^2 = 0.07$, $P = 0.38$), albumin concentration ($R^2 = 0.02$, $P = 0.91$), platelet count ($R^2 = 0.04$, $P = 0.65$), and hemoglobin concentration ($R^2 = 0.03$, $P = 0.25$) did not demonstrate any additional factors with a significant correlation with IC_{50} fold change, although concomitant medications were not accounted for and may represent a confounding hidden variable.

The Modified PIA Measures TKI-AGP Affinity

We examined the relationship of IC_{50} fold change and plasma protein concentration (see Supplementary Discussion for derivation), and demonstrated:

$$\Delta = K_A (P_0 - P_A) + 1$$

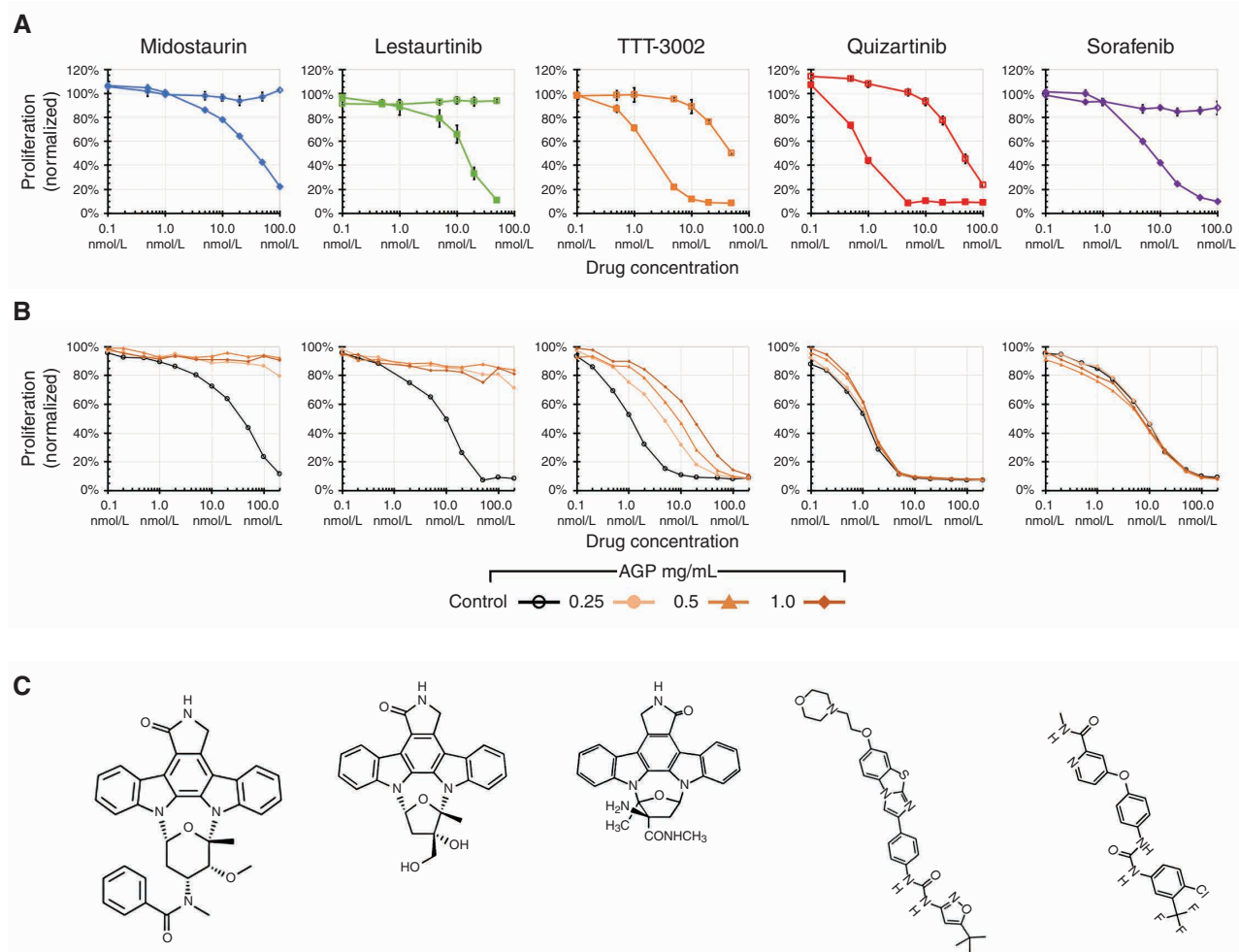


Figure 2. FLT3 inhibitors show variable inhibition by human plasma in both AGP-dependent and -independent fashions. MOLM-14 cells were exposed to increasing concentrations of the indicated FLT3 TKI under standard culture conditions (10% FBS) or in the presence of either 50% human plasma (A) or various concentrations of purified human AGP (0.25 mg/mL, 0.5 mg/mL, 1.0 mg/mL; B), and proliferation was measured by MTT after 48 hours. C, Structures of the various FLT3 TKIs used.

where Δ is the IC_{50} fold change, K_A is the drug-protein association constant, P_0 is the total protein concentration, and P_A is the drug-bound protein concentration. In the absence of other drug-protein interactions, fold change is linearly related to drug-free protein concentration. By using this relationship, comparing IC_{50} fold change to plasma AGP (Fig. 3A) yields biochemical data about the interaction of TKIs with their associated plasma protein. When the analysis takes into account drug-bound protein, these curves can be used to directly measure K_A . To that end, we performed the modified PIA using purified AGP against the staurosporine-derived FLT3 TKIs, using MOLM-14 cells (Fig. 4A). For comparison, we also assayed the antiproliferative effects of staurosporine upon HL-60 cells (FLT3 wild-type AML; refs. 21). Different TKIs show variable sensitivity to AGP inhibition ($P < 2 \times 10^{-16}$), with TTT-3002 being the least impacted (30-fold inhibition at physiologic concentrations), midostaurin showing intermediate inhibition (300-fold inhibition), and lestaurtinib

showing the highest (>1,000-fold inhibition predicted). In comparison, staurosporine demonstrated no appreciable activity in the presence of AGP until saturating concentrations of drug were used. Using regression analysis on the linear areas of these curves, we calculated binding constants for each drug (Fig. 4B). Of note, although midostaurin shows only intermediate levels of inhibition, when correcting for lower potency for FLT3 inhibition compared with lestaurtinib, the two drugs are predicted to have approximately the same *in vivo* activity (Supplementary Fig. S3).

To validate this approach as a quantitative assay, we also performed traditional competitive fluorescence displacement assays using 8-anilinonaphthalene-1-sulfonic acid (ANS), a polyaromatic compound that only fluoresces when bound to AGP (22). By measuring ANS fluorescence across a range of concentrations with fixed AGP, in the presence or absence of a competing drug of interest and then performing Scatchard analysis, we were able to use the Cheng-Prusoff

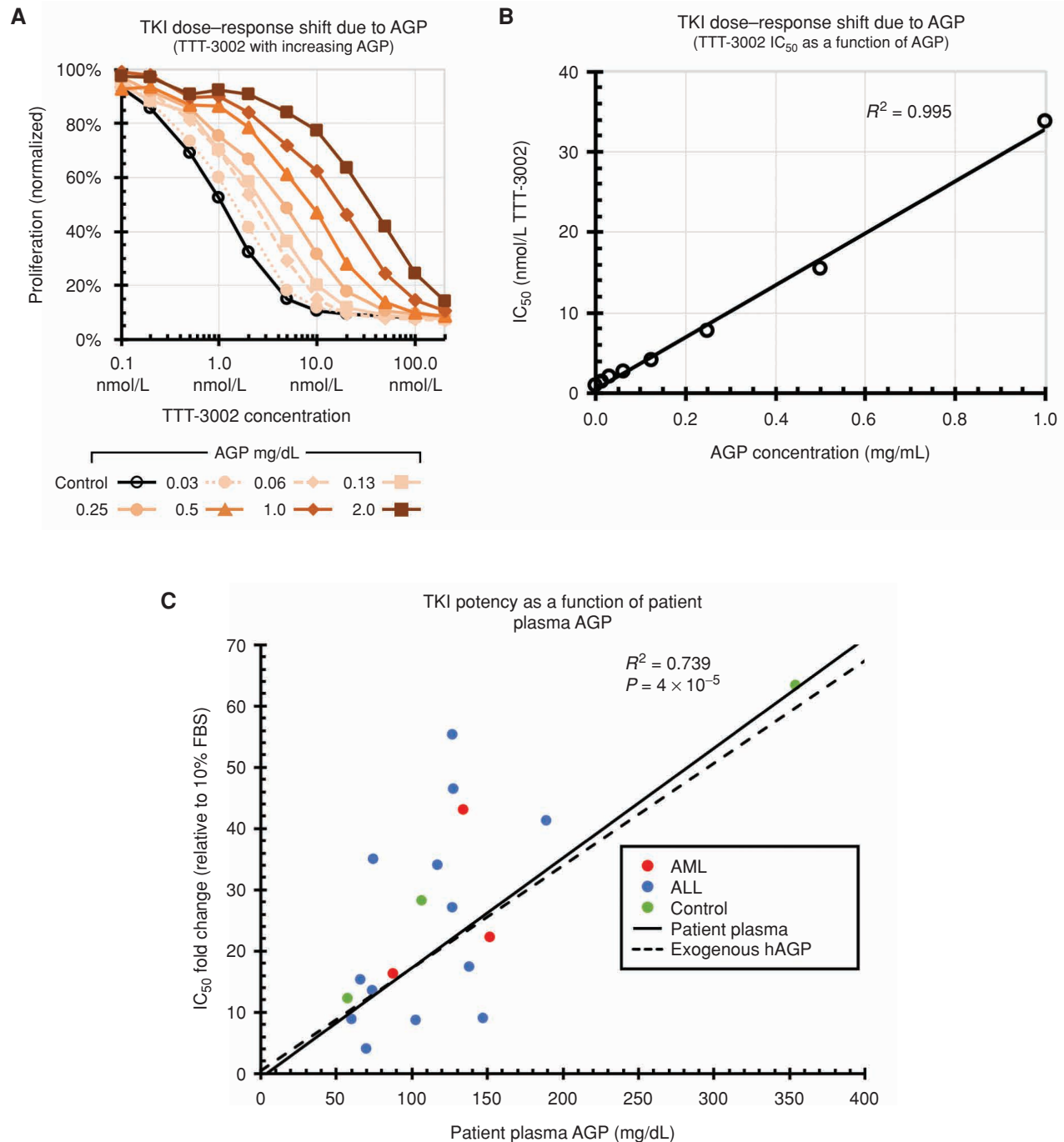


Figure 3. AGP demonstrates linear, dose-dependent inhibition of FLT3 TKI. **A**, MOLM-14 cells were cocultured in a range of concentrations of AGP (31 μ g/mL–2 mg/mL) and treated with increasing doses of the FLT3 TKI TTT-3002. Proliferation was measured by MTT after 48 hours. **B**, The IC_{50} for TTT-3002 was plotted as a function of AGP concentration. **C**, Plasma from 19 human patients was assayed for the ability to inhibit TTT-3002 using the modified PIA against MOLM-14 cells. The fold change in the IC_{50} (relative to cells treated under standard 10% FBS culture conditions) was calculated and plotted as a function of plasma AGP concentration as measured by radial immunodiffusion assay. Linear regression best fit is plotted (solid line) with the curve generated in **B** also plotted for comparison (dashed line). By convention, patient AGP concentration is reported as mg/dL.

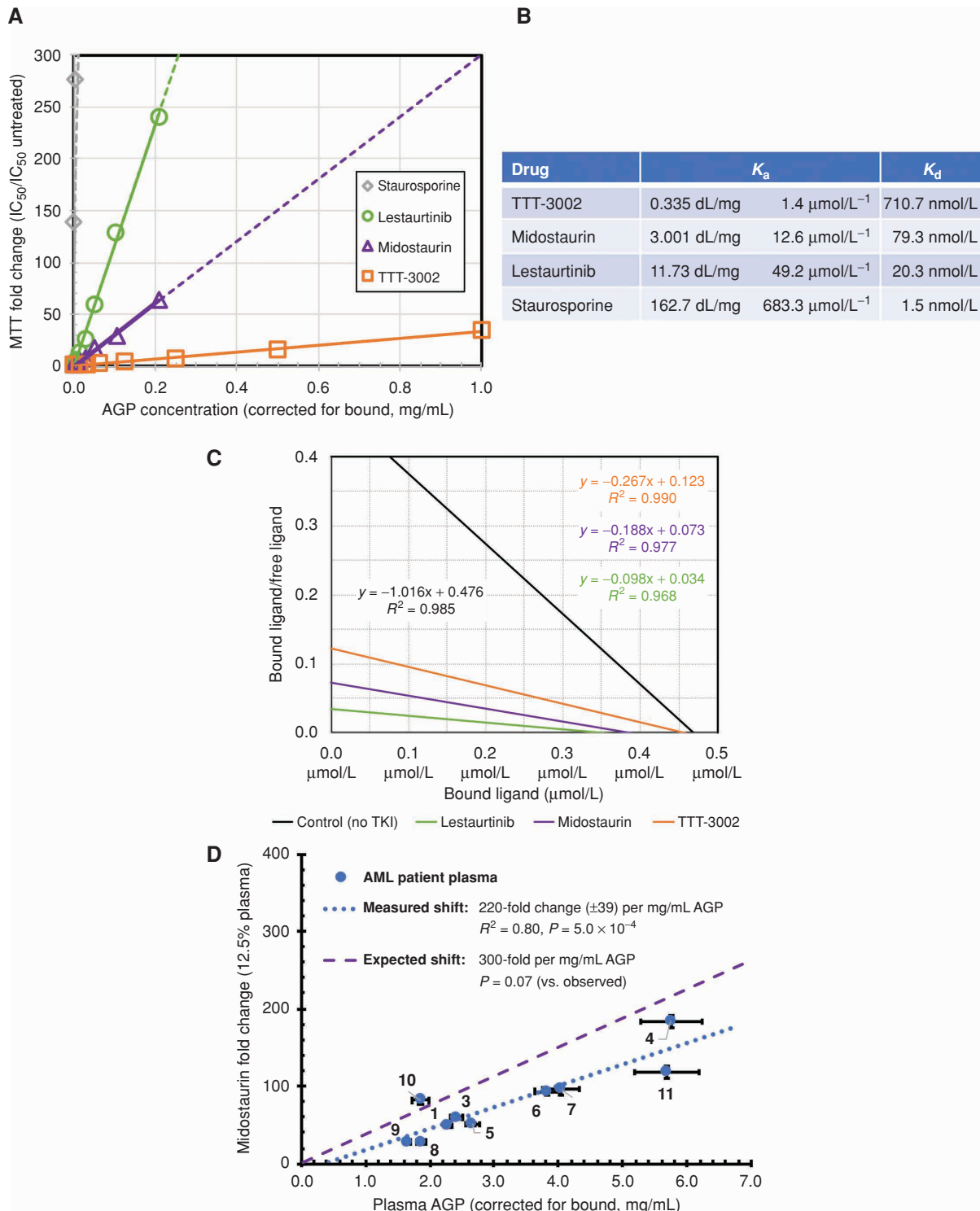


Figure 4. Human AGP binds staurosporine-derived FLT3 TKIs with variable affinities. **A**, MOLM-14 cells were cocultured in a range of concentrations of human AGP and treated with various staurosporine-derived FLT3 TKIs. The fold change in the IC_{50} (relative to cells treated under standard 10% FBS culture conditions) was calculated and plotted as a function of free AGP concentration (corrected for bound drug; IC_{50} with AGP - IC_{50} with 10% FBS). **B**, AGP binding constants for each drug were calculated from the linear regions of each curve (solid line); see text and Supplementary materials for mathematical treatment. **C**, Scatchard plots for fluorescence displacement assays examining competitive displacement of ANS from AGP by the indicated drugs. **D**, Plasma from 10 patients with newly diagnosed AML was assayed for the ability to inhibit midostaurin using the modified PIA against MOLM-14 cells. The fold change of IC_{50} in 12.5% plasma was calculated and plotted as a function of plasma AGP concentration (corrected for bound drug) as measured by ELISA. This was compared with the shift predicted by exogenous human AGP in **A** and **B**. Patient characteristics can be found in Supplementary Table S1.

approximation to measure drug-AGP affinity (Fig. 4C). These results were comparable with the results of the cell-based approach.

Finally, to demonstrate the clinical relevance of these findings, we collected samples from a second series of patients with newly diagnosed adult leukemia (Supplementary Table S1) and examined the effect of their plasma upon midostaurin activity. As expected, the modified PIA demonstrated significant loss in potency when coincubated in 12.5% human plasma (at higher concentrations, appreciable anti-FLT3 activity could not be quantitatively measured, unlike TTT-3002, which is not as severely shifted). This shift in IC_{50} followed a linear relationship with plasma AGP (Fig. 4D, only univariate analysis was performed on this group). For the lowest level AGP samples (patient 9, 1.67 mg/mL), even 12.5% plasma was sufficient to increase the IC_{50} 30-fold, and for about half of the patient samples, there was a 100-fold or greater shift in IC_{50} from nanomolar to the micromolar range. In 100% plasma, this would be expected to yield an IC_{50} of 10 to 20 $\mu\text{mol/L}$, with IC_{90-95} levels (i.e., the pharmacologic goal) 5-fold higher still. The patient plasma demonstrated a shift of 220-fold (± 39) per mg/mL AGP, which is similar to exogenous human AGP (300-fold per mg/mL, $P = 0.07$). Of note, this new diagnosis cohort had a 2.5-fold greater AGP level compared with the initial cohort (Fig. 3C, 270 ± 154 mg/dL vs. 117 ± 64 mg/dL, $P = 9 \times 10^{-4}$).

Overcoming Plasma Protein Inhibition with Mifepristone

The above assumes the absence of competitive drug-protein interactions. When we include a competitive binder of AGP (I), we find the fold-change/protein concentration relationship can be formulated as:

$$\Delta = \frac{K_A}{2K_I} \left(\beta - \gamma + \sqrt{(\beta - \gamma)^2 + 4\beta} \right) + 1$$

where:

$$\begin{aligned} \gamma &= K_I I_0 + 1 \\ \beta &= K_I \tau \end{aligned}$$

The derivation and a discussion of the significance of these relationships are described in the Supplementary Discussion. This relationship suggests that a competitor binding with comparable affinity to AGP will have a significant impact upon fold change, reducing the overall protein inhibition of the drug (Fig. 5A).

We undertook a proof-of-principle demonstration of disinhibiting FLT3 TKIs using unrelated drugs to displace TKIs. Of the known AGP-bound drugs, the steroid-derived estrogen receptor antagonist mifepristone has one of the highest association constants reported (22, 23). With a K_A of 7 to 8 $\mu\text{mol/L}$, it is predicted to bind to AGP with higher affinity than TTT-3002 and comparable affinity to lestaurtinib and midostaurin. Competitive fluorescence displacement confirms mifepristone displaces ANS from AGP at concentrations 1.5- to 2-fold lower than midostaurin and lestaurtinib (Fig. 5B). We performed the modified PIA using TTT-3002 and purified

AGP in the presence of increasing concentrations of mifepristone, and we found that the dose-response curve shifted back to that seen in the absence of AGP (Fig. 5C). Mifepristone had no impact upon the TTT-3002 dose-response curves in the absence of AGP. Furthermore, when we titrated mifepristone in the presence or absence of AGP and TKI, we found that growth inhibition of MOLM-14 cells by TKI in the presence of AGP was returned to that seen in the absence of AGP at concentrations of mifepristone comparable with those achieved in clinical trials (Fig. 5D; refs. 24–27). The maximal effect occurs at concentrations where mifepristone alone has no appreciable effect on cell growth. Similar effects were not seen using other known AGP-binding agents with lower affinities (Supplementary Fig. S4). These effects (Fig. 5E) agree within experimental limits to the model described above (Fig. 5A).

When MOLM-14 cells are treated with TTT-3002 in the presence of inhibiting concentrations of AGP, FLT3 inhibition is lost and derepression of downstream signaling is observed. Mifepristone alone has no effect upon FLT3 autophosphorylation or downstream signaling. However, the addition of mifepristone at increasing concentrations results in a dose-dependent restoration of FLT3 inhibition by TTT-3002 with loss of FLT3-dependent downstream signaling (Fig. 5F). This provides further support that mifepristone is acting through competitive displacement of TKIs from AGP, not off-target effects.

We hypothesized that among the various FDA-approved drugs and supplements, there exists a subset of agents that, like mifepristone, can bind AGP and displace bound TKIs, thus restoring anti-FLT3 activity. These agents might be used as combinatorial agents in restoring clinical activity of the staurosporine derivatives or serve as lead compounds for the development of such agents. Therefore, we screened the Johns Hopkins Drug Library (JHDL), a collection of 2,560 different agents approved for human or veterinary use. FLT3/ITD-expressing Ba/F3 cells were cocultured in cytotoxic concentrations of midostaurin (100 nmol/L) with inhibiting levels (0.5 mg/mL) of human AGP. To these, we added the various agents of the JHDL at 20 $\mu\text{mol/L}$ and measured cell growth by colorimetric means. To confirm that any cytotoxicity was FLT3 specific, and not a consequence of off-target activity by the JHDL compounds themselves, we performed parallel platings in the presence or absence of recombinant murine IL3. The IL3 (upon which the parental cells are dependent) will rescue the cells from FLT3-specific cytotoxicity, but not from off-target cytotoxicity. The majority of compounds had no impact upon cell growth or were equally cytotoxic in the presence or absence of IL3 (Fig. 6A). However, we identified 219 different agents that showed less cytotoxicity in the presence of IL3. Although approximately 30 compounds were still significantly cytotoxic in the presence of IL3 (Fig. 6A, area 2), the cytotoxicity of many of the compounds was mostly IL3 reversible (area 1). This subset of compounds may act by displacing midostaurin from AGP and restoring its anti-FLT3 activity.

To further screen these agents, we performed competitive fluorescence displacement with the JHDL compounds. We measured the relative fluorescence intensity of AGP-bound ANS in the presence of the different agents, normalizing

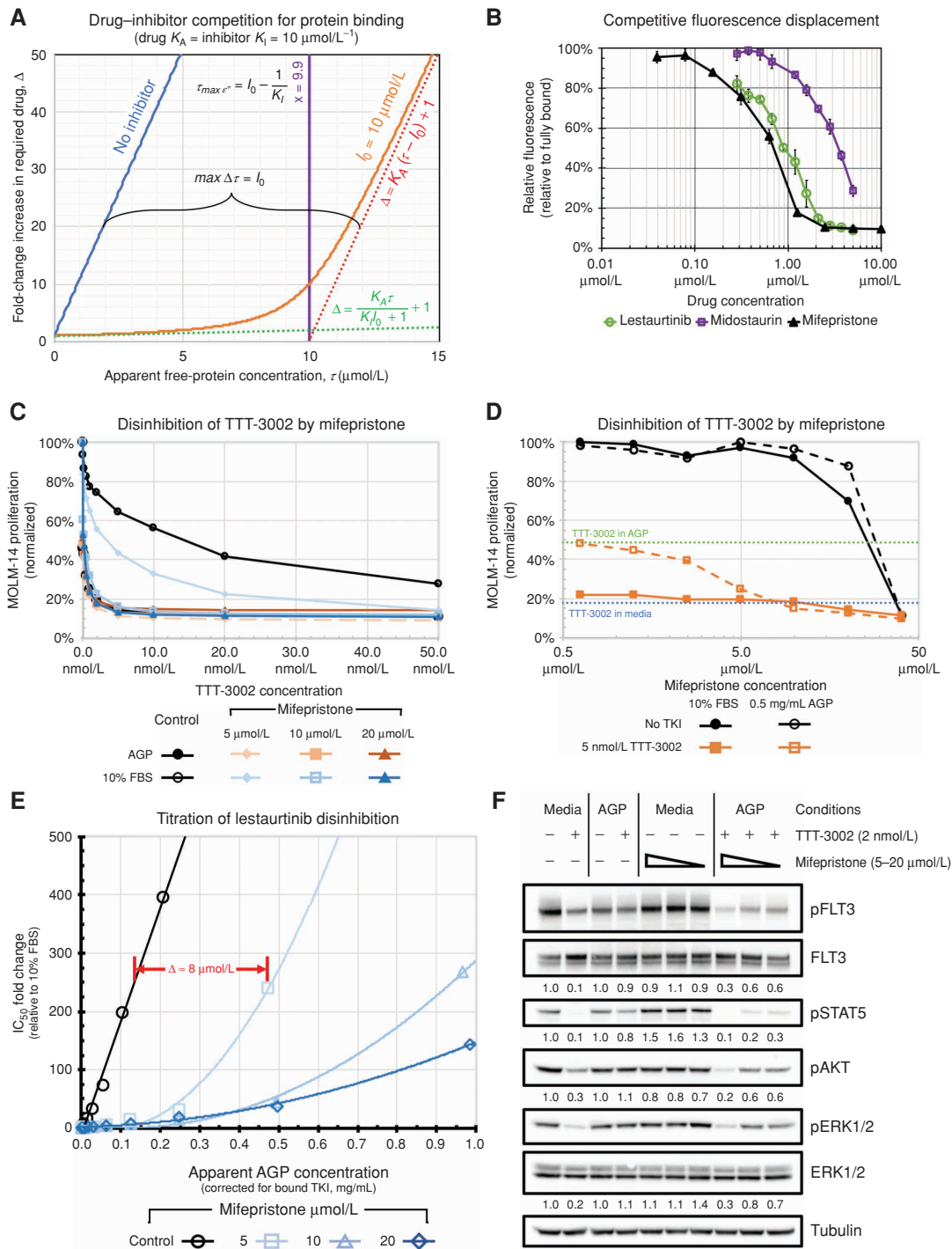


Figure 5. Inhibition of drug-protein binding is dependent upon protein and protein binding inhibitor characteristics and concentrations and can be abrogated by the addition of competitor compounds. **A**, Key aspects of the fold-change growth inhibition curves generated using an idealized drug ($K_A = 10 \mu\text{mol/L}^{-1}$) and a binding inhibitor ($K_I = 10 \mu\text{mol/L}^{-1}$, $I_0 = 10 \mu\text{mol/L}$). Growth inhibition curves are shown for both the presence (orange) and absence (blue) of a binding inhibitor. Shown are the curves and equations for the asymptotes at low (green) and high (red) protein concentrations, the apparent free-protein concentration (purple) at which the curve has the greatest rate of increasing slope, and the maximal shift (bracket) in the curve caused by the presence of a binding inhibitor. **B**, Competitive fluorescence displacement was performed in the presence of increasing concentrations of AGP-binding drugs (lestaurtinib, midostaurin, mifepristone). ANS only exhibits fluorescence when bound to AGP. **C**, Dose-response curves using the modified PIA in the presence of increasing doses of mifepristone, a potential binding inhibitor, show a return of the curves toward those seen under standard culture conditions (10% FBS) despite the presence of inhibitory levels of AGP. **D**, Coincubation of MOLM-14 cells with mifepristone restores TTT-3002 activity (5 nmol/L) in the presence of AGP in a mifepristone dose-dependent manner. **E**, The effect, as modeled in **A**, was experimentally measured in MOLM-14 cells as the fold change in IC_{50} of lestaurtinib for cells cocultured with varying concentrations of mifepristone (15 $\mu\text{mol/L}$, 10 $\mu\text{mol/L}$, 5 $\mu\text{mol/L}$) and AGP (2-fold dilutions from 1 mg/mL to 3.9 $\mu\text{g/mL}$, where 1 mg/mL \approx 20 $\mu\text{mol/L}$ AGP). **F**, MOLM-14 cells were treated with TTT-3002 (2 nmol/L) in the presence or absence of inhibitory levels of AGP; the effect of coincubation with mifepristone upon FLT3/ITD signaling inhibition was measured through phospho-Western blot analysis.

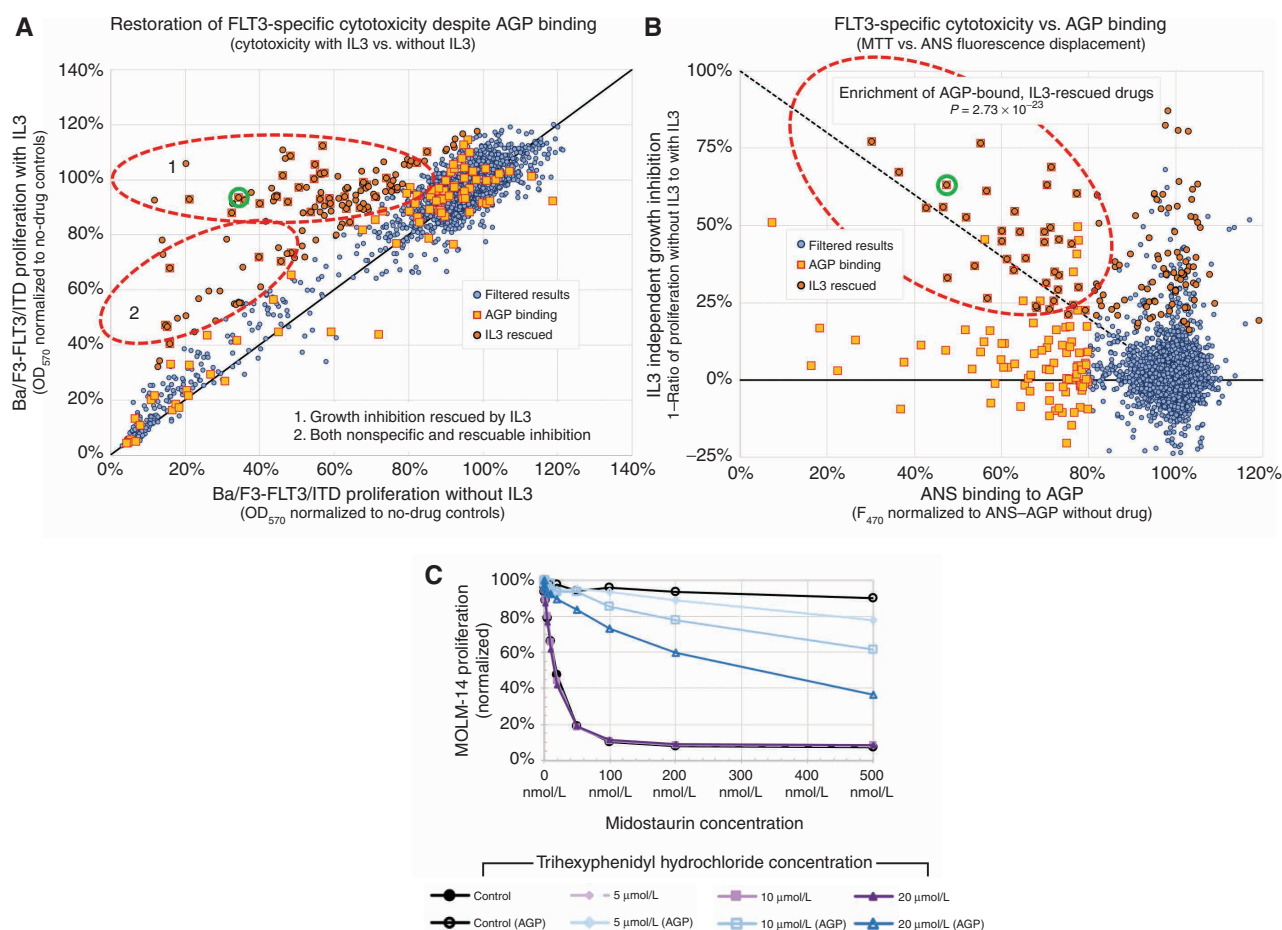


Figure 6. Identification of compounds that can restore TKI activity despite inhibitory levels of AGP. **A**, Ba/F3-FLT3/ITD cells were exposed to cytotoxic concentrations of midostaurin (100 nmol/L) in the presence of inhibitory levels of AGP (0.5 mg/mL) and cocultured with a library of 2,800 FDA-approved drugs with or without 1 ng/mL of IL3. After 48 hours in culture, cell growth was assessed by the MTT colorimetric assay and growth in IL3 was plotted against growth in its absence. Candidate compounds are those that show cytotoxicity that can be completely (area 1) or partially (area 2) rescued by IL3. **B**, Compounds were also measured for their ability to displace AGP-bound ANS, and IL3-rescueable growth inhibition was plotted as a function of ANS binding to AGP. Compounds that both displace ANS from AGP and restore IL3-rescueable cytotoxicity are enclosed in the red dashed region. **C**, Validation of one candidate compound, trihexyphenidyl hydrochloride. Cotreatment with increasing doses (indicated in legend) results in increasing TKI activity despite the presence of inhibitory (1 mg/mL) AGP. Its position on plots **A** and **B** is indicated by a green circle.

to intensity in the absence of competing drug. When IL3-independent growth inhibition (1 minus the ratio of growth in the absence and presence of IL3) is compared with ANS displacement (Fig. 6B), several classes of agents are identified. The majority of agents ($n = 2,343$) have neither FLT3-specific growth-inhibitory nor AGP-binding activities, while a small subset of agents ($n = 88$) bind to AGP but are unable to restore anti-FLT3 activity. Interestingly, a small group of agents ($n = 91$, upper-right quadrant) do not appear to bind to AGP (at least not competitively with ANS), but nonetheless induce cytotoxicity that is IL3 reversible. It is possible that these agents have intrinsic anti-FLT3 activity, or that they are synergistic with midostaurin such that the low levels of FLT3 inhibition present are now sufficient to induce cytotoxicity by either targeting alternative pathways or directly targeting downstream signaling pathways. In addition, a group of 38 agents (indicated by the dashed ellipse, upper-left quadrant) are able to both bind to AGP and restore anti-FLT3 activity. There are 6-fold more agents in this fourth group than would be expected based upon

the number of agents found in the other groups (38 identified vs. 6.3 expected, $P = 2.73 \times 10^{-23}$, Fisher exact test). An initial validation of the 10 lead compounds demonstrated at least one, trihexyphenidyl hydrochloride, that is able to improve midostaurin activity in the presence of inhibiting AGP concentrations (Fig. 6C) to an extent similar to the effects seen with mifepristone (Fig. 5C). Testing of other candidates is in progress.

We performed an *in vivo* proof-of-principle of competitive disinhibition of TKIs in mice (Fig. 7A). Murine AGP has very limited homology to human AGP and is expressed at levels 5- to 10-fold lower than humans, and work in rats has demonstrated physiologically significant differences between human and rodent AGP (28). Therefore, we created a mouse model for testing the effects of human AGP *in vivo*. Mice injected with human AGP at 0.3 g/kg i.p. every 48 hours demonstrated serum AGP levels ranging from 0.5 to 3 mg/mL (Fig. 7B), with a terminal half-life of approximately 17 hours. Consistent with previous work in rats, mice did not demonstrate any appreciable toxicities from this administration

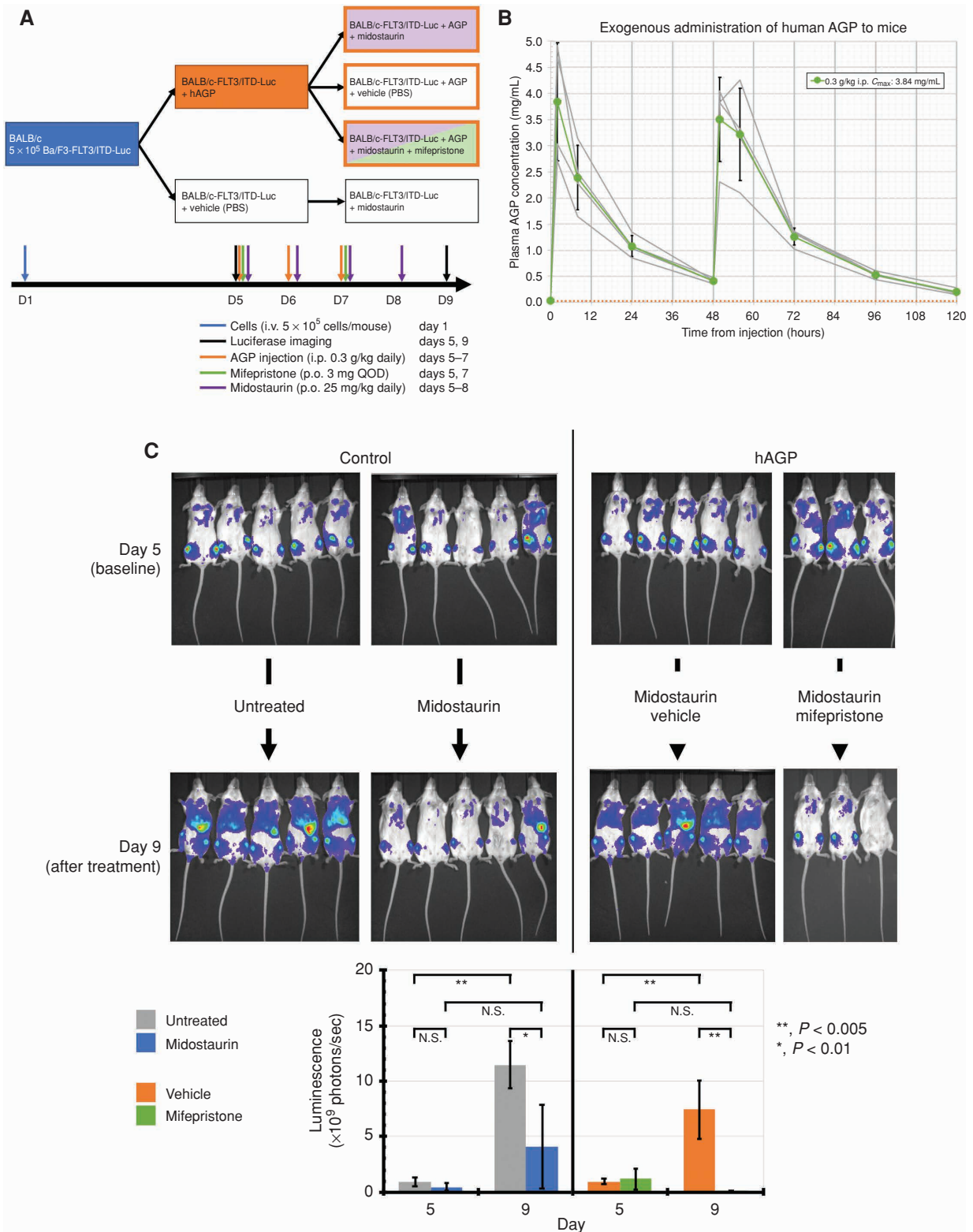


Figure 7. Human AGP inhibits midostaurin efficacy and can be rescued by mifepristone *in vivo*. **A**, Experimental scheme. QOD, every other day. **B**, Human AGP was injected intraperitoneally at 0 and 48 hours, and the plasma concentration was measured at various time point via human-specific ELISA. Green line indicates the average of four independent mice (gray lines). **C**, Sublethally irradiated BALB/c mice were engrafted with 5×10^5 Ba/F3-FLT3/ITD-Luc cells. Bioluminescent imaging on day 5 confirmed engraftment. After engraftment, recipients received human AGP or vehicle by intraperitoneal injection, and either midostaurin or vehicle by oral gavage for 4 days. A subgroup of hAGP/midostaurin mice also received mifepristone by oral gavage. Response was assessed on day 9 by repeat bioluminescent imaging. Shown is a representative example of duplicate runs. Average radiance is plotted with significant differences indicated (**, $P < 0.005$, *, $P < 0.01$, $\alpha = 0.05$, bars indicate SD). N.S., not significant.

over the 2 weeks they were observed. We transplanted sublethally irradiated BALB/c mice with Ba/F3-FLT3/ITD-Luc cells (expressing both FLT3/ITD and a luciferase reporter). After 5 days, luciferin bioluminescence confirmed adequate engraftment (Fig. 7C). The mice were then treated with orally gavaged midostaurin or vehicle for 4 days. At the same time, a subset of the midostaurin-treated mice were also conditioned with intraperitoneal human AGP or AGP plus oral mifepristone. The remaining were injected with PBS vehicle. Twenty-four hours after the final treatment (day 9), the mice were again imaged (Fig. 7C). All mock-treated mice demonstrated progression of the FLT3/ITD-expressing cells, whereas the mice treated with midostaurin alone showed regression of the cells over the treatment course. However, treated mice that received intraperitoneal AGP demonstrated progression of the cells comparable with that seen in the control animals. In contrast, when the midostaurin/AGP dual-treated mice were also gavaged mifepristone daily during treatment, the mice again demonstrated regression of the transplanted cells comparable with those of the midostaurin alone-treated mice.

DISCUSSION

Since the discovery of FLT3 and its associated activating mutations, it has remained a consistent target for drug development (29). Two approaches, rational drug design and library-based screening, have been used for the discovery of new anti-FLT3 agents, with subsequent generations demonstrating increasing potency *in vitro*. These agents tend to be either staurosporine derivatives, such as midostaurin and lestaurtinib, or are complex polyaromatic compounds, such as gilteritinib, quizartinib, and sorafenib. Staurosporines tend to be very potent, possibly due to additional off-target inhibition of targets such as PKC. They are also active against the FLT3 kinase domain mutations that have been associated with resistance to some of the FLT3 TKIs that have no activity against such mutations. However, they have significant dose-limiting toxicities, especially gastrointestinal, likely due to the same off-target effects. In contrast, some non-staurosporine agents, with more selective anti-FLT3 activity, often demonstrate higher *in vitro* IC₅₀s (i.e., reduced potency) and can be inhibited by more resistance-associated point mutations, but tend to be less dose limited (30). Yet, despite this wide selection of diverse inhibitors spanning two decades, clinical trials have often fallen short of the expectations of preclinical work. In addition to prior concerns for resistance mutations, we believe that the results presented here highlight an underappreciated pitfall in the development of drugs for FLT3 AML that is likely contributing to their clinical underperformance.

One particularly informative FLT3 TKI clinical trial was that of lestaurtinib for relapsed FLT3-mutant AML (31–33). There, the addition of lestaurtinib to standard induction therapy failed to improve response rates or overall survival. This was despite *in vitro* potency and patients achieving plasma drug levels nearly 1,000-fold higher than necessary for *in vitro* cytotoxicity. When patient plasma samples were directly tested for the ability to inhibit FLT3 using the original PIA, most samples failed to demonstrate sufficient levels (>90%) of inhibitory activity. However, for

those patients whose samples did achieve high levels of FLT3 inhibitory activity, there was an increase in attaining a complete remission. FLT3-inhibitory activity did not always correlate with plasma drug levels (9). The dissociation of drug activity from level (pharmacodynamics from pharmacokinetics) was the earliest suggestion that FLT3 TKI therapy is greatly modulated by drug availability within the plasma compartment. The results presented here provide a mechanistic explanation whereby the predicted IC₅₀ is significantly higher than most of the levels seen in patients despite excellent total drug levels.

Concerns regarding the effect of host factors on FLT3 TKI therapy have also been raised in response to the recent trial that led to the FDA approval of midostaurin. Midostaurin added to standard induction therapy yielded a modest but significant improvement in overall survival for patients regardless of FLT3 mutational type or burden (34). Yet these different FLT3-mutant disease subtypes have been demonstrated to be clinically and biologically very distinct entities, not equally dependent upon FLT3 (1, 3, 35–38). Relapse data suggest that in some patients, there is nonetheless selective pressure from anti-FLT3 activity (39). However, our data indicate that for many patients, midostaurin would have adequately cytotoxic anti-FLT3 activity only at concentrations significantly higher than drug levels typically achieved in clinical trials. This suggests that its potent *in vitro* anti-FLT3 activity is significantly attenuated if not largely lost *in vivo*, and survival benefits may be through non-FLT3 effects, especially in non-ITD disease. This is consistent with findings that midostaurin inhibits a multitude of targets in the kinome and may even have general antileukemic effects (40, 41).

The drug-binding effects demonstrated in this report are not limited to AML. At least two other trials have experienced significant complications due to the drug-binding effects of AGP. Trials with 7-hydroxy-staurosporine for refractory neoplasms demonstrated disappointing results despite promising preclinical results (14, 15, 42). Pharmacologic work identified drug binding to AGP as having been a complicating factor not predicted in preclinical models (43, 44). A separate trial using the non-staurosporine TKI filanesib for relapsed and refractory multiple myeloma met with similar results (16, 17). The filanesib trial demonstrated a clear association between plasma AGP concentration and response, with the few responders having the lowest AGP concentrations of the cohort. Further complicating the clinical picture, natural AGP variants can have even greater effects upon drug activity (45, 46). Finally, as an acute-phase reactant, AGP concentration is highly variable in disease states such as AML (12, 18). Indeed, our new-diagnosis validation cohort demonstrated markedly higher AGP levels compared with the initial cohort comprised of control and postinduction samples. Although this study did not specifically examine the relationship between AGP concentration and disease state, it is intriguing to think that AGP could be used as a biomarker to select either specific TKI or combinatorial approaches for patients.

These effects are not new; FDA approval involves assaying protein binding, and the literature has many similar “rediscoveries” of the problem of plasma protein binding

(47–49). As drug development becomes more specialized, the health and economic consequences of ignoring drug-binding effects during the preclinical stage of drug development and until they are observed in the clinical setting can be significant. The work presented here indicates that significant species-specific differences in homology and expression levels of plasma proteins masks these effects in tissue culture and animal models. Even mouse models designed to study AGP binding utilize nonhuman constructs and could thus fail to predict binding and subsequent failure of the drugs in clinical trials (50, 51). Our data show that bovine AGP, even when adjusted to human-comparable levels, produces an approximate 5-fold IC_{50} increase for lestaurtinib, the most tightly bound of the staurosporines, compared with the 500-fold shift produced by human AGP. This mirrors prior work that demonstrated a protective effect of human AGP in reperfusion injury that is not found with mouse AGP (28). Furthermore, cow and mouse plasma contain significantly lower AGP concentrations (2- to 10-fold lower) compared with human plasma (18, 20). These findings indicate the need for new models to study drug-protein binding that faithfully recapitulate human-specific effects. To our knowledge, this is the first time such a model has been demonstrated for drug testing and represents an exciting new platform for drug development. In the meantime, it is critical for investigators and drug developers to be aware of the limitations of current models and implement testing such as the modified PIA to avoid these failures.

Using a second drug to increase the free-drug concentration of target drugs to levels that are able to more fully inhibit the intended target is one way to potentially increase efficacy. In addition, by indirectly increasing drug potency, it may be possible to reduce drug dose. This may lead to reduced gastrointestinal exposure and potentially reduce one of the most significant dose-limiting toxicities observed in clinical trials. Thus, it may be possible to decrease drug dose while nonetheless improving efficacy. Although testing and validation continue, our screen has demonstrated that other agents exist with properties similar to mifepristone, and such agents could either form the basis of future combinatorial clinical trials or serve as lead compounds to new, biologically inactive plasma protein “decoys.” Indeed, even if none of these agents prove to be feasible for clinical use, this new method of screening agents and probing the drug-protein interaction space should provide a wealth of information regarding drug structure-protein interaction to inform the development of new decoys and future drug development (i.e., chemical motifs best avoided during drug development). It is encouraging that mifepristone, a drug that is highly specific for the estrogen receptor, with few off-target effects, has shown promise both *in vitro* and *in vivo*. This suggests that this FDA-approved drug may itself be a candidate for use in an early-phase trial to develop this combinatorial approach for overcoming plasma protein binding. Through better awareness of drug-protein interactions, newer models for studying the effects, and the use of combinatorial therapeutic approaches, it may be possible to finally realize the potential of targeted therapies for *FLT3*-mutant AML and for other diseases where molecularly targeted therapies have failed to achieve their full promise.

METHODS

Patient Plasma

Unless otherwise specified, pooled plasma from healthy donors was used for all experiments. Patient samples were collected from patients seen in the pediatric oncology clinic at Johns Hopkins Hospital between November 2015 and March 2016. Patients were enrolled in an Institutional Review Board-approved, institutional banking protocol with written informed patient consent in accordance with the Declaration of Helsinki. Whole blood was collected by venipuncture in sodium heparin-treated vacutainer tubes (BD Biosciences). Within 2 hours of collection, cellular components were separated from the plasma by centrifugation twice at $2,000 \times g$ for 10 minutes, stored until use at $-80^{\circ}C$, and clarified immediately prior to use by centrifugation at $\geq 15,000 \times g$ for 3 minutes. Plasma AGP concentrations were measured by radial immunodiffusion assay (Kent Labs) according to the manufacturer's protocols.

Reagents

AGP purified from human or bovine plasma (Sigma) was resuspended in unsupplemented RPMI1640 (Gibco) at 10 mg/mL for working stocks. Recombinant human serum albumin (Sigma) was resuspended in RPMI1640 at 100 mg/mL. Lyophilized bovine plasma (Sigma) was reconstituted in sterile PBS (Gibco). TTT-3002 was a generous gift of TauTaTis, Inc. Lestaurtinib, midostaurin, sorafenib, and quizartinib were purchased from LC Laboratories. Each *FLT3* TKI was dissolved at 10 mmol/L in 100% sterile-filtered dimethylsulfoxide (DMSO, Sigma). Mifepristone (Sigma) was dissolved at 100 mmol/L in 100% DMSO. Trihexyphenidyl hydrochloride (Selleckchem) was dissolved at 100 mmol/L in methanol. For cell-based assays, working stocks of 10 μ mol/L were prepared for each drug in RPMI1640 supplemented with 0.1% DMSO and 0.2% BSA. For spectrophotometric studies, working stocks of 10 μ mol/L were prepared using PBS without sera or albumin. ANS (Sigma) was dissolved in DMSO at 200 mmol/L and then diluted to 400 μ mol/L with PBS (0.2% DMSO, final). Western blot analysis was performed using the *FLT3* S-18 antibody (Santa Cruz Biotechnology) and for other proteins as indicated (Cell Signaling Technology).

Cell Lines

Unless otherwise stated, MOLM-14 cells (DSMZ catalog no. ACC-777, RRID:CVCL_7916) and Ba/F3 (DSMZ, catalog no. ACC-300, RRID:CVCL_0161) were grown in RPMI1640 media, supplemented with 10% heat-inactivated FBS (Gemini), with antibiotics. The Ba/F3-*FLT3*/ITD cell line is a Ba/F3 cell line into which the neomycin-selectable pBABE vector with *FLT3*/ITD has been stably incorporated as described previously (30, 52). The Ba/F3-*FLT3*/ITD-Luc cell line was the Ba/F3 *FLT3*/ITD cells transfected with the L3-3GFP plasmid containing genes for luciferase and GFP (52). Parental Ba/F3 cells were cultured with 1 ng/mL recombinant mouse IL3, whereas Ba/F3-*FLT3*/ITD and Ba/F3-*FLT3*/ITD-Luc cells were maintained without supplemental cytokines. Cells were maintained at 4×10^5 to 2×10^6 cells per milliliter and cultured in humidified, $37^{\circ}C$ incubators, with 5% carbon dioxide. All cell line work was performed using *Mycoplasma*-free (confirmed by PCR) stocks and used within 1 month of thawing (approximately 12 passages).

Modified PIA

Cells in logarithmic growth were resuspended in either human plasma or serum-free RPMI1640 media supplemented with the plasma protein of interest and seeded in 96-well format at 50 μ L per well. Cell density was 2×10^5 cells per well for MOLM-14 and Ba/F3-*FLT3*/ITD cells. To each well, 50 μ L of 2 \times drug dilution in RPMI1640 media with 10% serum was added. Each condition was plated in quadruplicate. The cells were then incubated at $37^{\circ}C$. After

44 hours of treatment, 10 μ L of 5 mg/mL thiazolyl blue tetrazolium bromide (MTT, Sigma) in PBS, sterile-filtered, was added to each well, and the plates were incubated for an additional 4 hours at 37°C. One-hundred microliters of 10% SDS (JT Baker) in 10 mmol/L hydrochloric acid (Thermo Fisher Scientific) was then added to each well, and the plates were incubated at 37°C overnight. Optical absorbance at 570 nm was measured via a plate reader (iMark, Bio-Rad), averaging across technical replicates. Fifty percent inhibition of proliferation (IC_{50}) values was calculated by linear regression analysis relative to cells cultured without drug(s) in the corresponding presence or absence of plasma or plasma proteins.

Fluorescence Displacement Titration

Drug affinity was measured by displacement of ANS from AGP using the previously described fluorescent spectrophotometric method (22). The drug of interest, dissolved in serum-free PBS, was combined with AGP and ANS for final concentrations of 1 μ mol/L drug, 0.5 mg/mL AGP and ANS at a range of 90 nmol/L to 50 μ mol/L. Drugs and protein were allowed to equilibrate in the dark at room temperature for 2 hours. Fluorescence was measured (emission 470 nm, excitation 400 nm) with a SpectraMax M3 Multi-Mode Microplate reader (Molecular Devices). Maximal fluorescence was determined by measuring ANS fluorescence in the presence of 100 μ mol/L human serum albumin (Sigma) without drug. Bound ANS was calculated as the product of total ANS concentration times the fraction of maximal fluorescence observed. The K_A of ANS with AGP in the absence of drug was calculated by Scatchard analysis, and the binding constants were determined by the Cheng-Prusoff approximation.

Animal Studies

BALB/c (IMSR catalog no. JAX:000651, RRID:IMSR_JAX:000651) mice were sublethally X-ray irradiated with 300 cGy (CIXD irradiator, Xstrahl) and injected with 5×10^5 Ba/F3-FLT3/ITD-Luc cells via tail vein. Intraperitoneal injections were performed using PBS vehicle with human AGP (Sigma) at 20 mg/mL. Midostaurin was suspended in 30% (w/v) Cremophor EL, 30% (w/v) PEG 400, 10% ethanol, and 10% glucose (all Sigma) and instilled once daily by oral gavage (10, 11). These drug doses have previously been demonstrated to be effective in mice. Mifepristone (Sigma) was dissolved in 50% ethanol and 50% (2-hydroxypropyl)- β -cyclodextrin (Sigma) and gavaged every 48 hours. Mice were imaged by intraperitoneal injection of luciferin (3 mg) and visualized on an IVIS Spectrum imager (Caliper LifeSciences) using Living Image software for analysis on day 5 (to monitor engraftment) and on day 9 (to assess drug effect). Animal husbandry and procedures were conducted in accordance with the policy of the Johns Hopkins University School of Medicine Animal Care and Use Committee.

Authors' Disclosures

D.J. Young reports nonfinancial support from Novartis outside the submitted work, as well as a patent for US/2021/0154208A1 pending. M.J. Levis reports grants and personal fees from Astellas and Takeda, grants from FujiFilm, and personal fees from AbbVie, Amgen, Daiichi Sankyo, Bristol Myers Squibb, Jazz, and Pfizer during the conduct of the study, as well as receiving research support from and serving as a consultant for Novartis outside the submitted work. J.O. Liu reports a patent for method to identify agents that can overcome inhibition caused by drug-protein binding of the human plasma protein, alpha-1-acid glycoprotein (US/2021/0154208A1), pending, for which a patent application has been filed by Johns Hopkins. D. Small reports grants from NCI (CA090668 and P30 CA006973), Alex's Lemonade Stand, Giant Food Pediatric Cancer Fund and other support from Kyle Haydock Professorship during the conduct of the study; grants and personal fees from Pharos

I&BT Co., Ltd. outside the submitted work; a patent for a method for overcoming plasma protein inhibition of tyrosine kinase inhibitors (US/2021/0154208A1) pending; serves on the scientific advisory board for InSilico Medicine and receives research support and serves as a consultant for an unrelated project from Pharos I&BT Co., Ltd. This arrangement has been reviewed and approved by the Johns Hopkins University in accordance with its conflict of interest policies. No disclosures were reported by the other authors.

Authors' Contributions

D.J. Young: Conceptualization, formal analysis, investigation, methodology, writing—original draft. **B. Nguyen:** Formal analysis, funding acquisition, validation, investigation, methodology, writing—review and editing. **L. Li:** Formal analysis, validation, investigation, methodology, writing—review and editing. **T. Higashimoto:** Formal analysis, investigation, methodology. **M.J. Levis:** Resources, formal analysis, investigation, methodology, writing—review and editing. **J.O. Liu:** Resources, formal analysis, investigation, methodology, writing—review and editing. **D. Small:** Resources, formal analysis, supervision, funding acquisition, methodology, writing—review and editing.

Acknowledgments

This work was supported by NIH grants (R01 CA090668 and P30 CA006973), a grant from Alex's Lemonade Stand (to D. Small) and the Giant Food Pediatric Cancer Fund. D.J. Young is supported by the NIH Fellowship for Pediatric Oncology (T32 CA060441) and the Optimist Foundation Fellowship. The Johns Hopkins Drug Library was also supported in part by FAMRI (to J.O. Liu). D. Small is also supported by the Kyle Haydock Professorship.

Received July 1, 2020; revised November 2, 2020; accepted June 29, 2021; published first July 2, 2021.

REFERENCES

- Levis M, Small D. FLT3: ITD does matter in leukemia. *Leukemia* 2003;17:1738–52.
- Patel JP, Gonen M, Figueroa ME, Fernandez H, Sun Z, Racevskis J, et al. Prognostic relevance of integrated genetic profiling in acute myeloid leukemia. *N Engl J Med* 2012;366:1079–89.
- Kottaridis PD, Gale RE, Frew ME, Harrison G, Langabeer SE, Belton AA, et al. The presence of a FLT3 internal tandem duplication in patients with acute myeloid leukemia (AML) adds important prognostic information to cytogenetic risk group and response to the first cycle of chemotherapy: analysis of 854 patients from the United Kingdom Medical Research Council AML 10 and 12 trials. *Blood* 2001;98:1752–9.
- Chu SH, Heiser D, Li L, Kaplan I, Collector M, Huso D, et al. FLT3-ITD knockin impairs hematopoietic stem cell quiescence/homeostasis, leading to myeloproliferative neoplasm. *Cell Stem Cell* 2012;11:346–58.
- Gilliland DG, Griffin JD. The roles of FLT3 in hematopoiesis and leukemia. *Blood* 2002;100:1532–42.
- Mizuki M, Fenski R, Halfter H, Matsumura I, Schmidt R, Muller C, et al. Flt3 mutations from patients with acute myeloid leukemia induce transformation of 32D cells mediated by the Ras and STAT5 pathways. *Blood* 2000;96:3907–14.
- Hayakawa F, Towatari M, Kiyoi H, Tanimoto M, Kitamura T, Saito H, et al. Tandem-duplicated Flt3 constitutively activates STAT5 and MAP kinase and introduces autonomous cell growth in IL-3-dependent cell lines. *Oncogene* 2000;19:624–31.
- Tse KF, Novelli E, Civin CI, Bohmer FD, Small D. Inhibition of FLT3-mediated transformation by use of a tyrosine kinase inhibitor. *Leukemia* 2001;15:1001–10.

9. Levis M, Brown P, Smith BD, Stine A, Pham R, Stone R, et al. Plasma inhibitory activity (PIA): a pharmacodynamic assay reveals insights into the basis for cytotoxic response to FLT3 inhibitors. *Blood* 2006;108:3477–83.
10. Ma H, Nguyen B, Li L, Greenblatt S, Williams A, Zhao M, et al. TTT-3002 is a novel FLT3 tyrosine kinase inhibitor with activity against FLT3-associated leukemias in vitro and in vivo. *Blood* 2014;123:1525–34.
11. Ma HS, Nguyen B, Duffield AS, Li L, Galanis A, Williams AB, et al. FLT3 kinase inhibitor TTT-3002 overcomes both activating and drug resistance mutations in FLT3 in acute myeloid leukemia. *Cancer Res* 2014;74:5206–17.
12. Fournier T, Medjoubi NN, Porquet D. Alpha-1-acid glycoprotein. *Biochim Biophys Acta* 2000;1482:157–71.
13. Kremer JM, Wilting J, Janssen LH. Drug binding to human alpha-1-acid glycoprotein in health and disease. *Pharmacol Rev* 1988;40:1–47.
14. Fuse E, Tanii H, Kurata N, Kobayashi H, Shimada Y, Tamura T, et al. Unpredicted clinical pharmacology of UCN-01 caused by specific binding to human alpha-1-acid glycoprotein. *Cancer Res* 1998;58:3248–53.
15. Fuse E, Tanii H, Takai K, Asanome K, Kurata N, Kobayashi H, et al. Altered pharmacokinetics of a novel anticancer drug, UCN-01, caused by specific high affinity binding to alpha-1-acid glycoprotein in humans. *Cancer Res* 1999;59:1054–60.
16. Tunquist B, Brown K, Hingorani G, Lonial S, Kaufman JL, Zonder JA, et al. Identification of alpha 1-acid glycoprotein (AAG) as a potential patient selection biomarker for improved clinical activity of the novel KSP inhibitor ARRY-520 in relapsed and refractory multiple myeloma (MM). *Blood* 2012;120:1868.
17. Shah JJ, Zonder J, Bensingier WI, Cohen AD, Kaufman JL, Nooka AK, et al. Prolonged survival and improved response rates with ARRY-520 in relapsed/refractory multiple myeloma (RRMM) patients with low α -1 acid glycoprotein (AAG) levels: results from a phase 2 study. *Blood* 2013;122:285.
18. Hocheppied T, Van Molle W, Berger FG, Baumann H, Libert C. Involvement of the acute phase protein alpha 1-acid glycoprotein in nonspecific resistance to a lethal gram-negative infection. *J Biol Chem* 2000;275:14903–9.
19. Kopf M, Baumann H, Freer G, Freudenberg M, Lamers M, Kishimoto T, et al. Impaired immune and acute-phase responses in interleukin-6-deficient mice. *Nature* 1994;368:339–42.
20. Tamura K, Yatsu T, Itoh H, Motoi Y. Isolation, characterization, and quantitative measurement of serum alpha 1-acid glycoprotein in cattle. *Nihon Juigaku Zasshi* 1989;51:987–94.
21. Jarvis WD, Turner AJ, Povirk LF, Traylor RS, Grant S. Induction of apoptotic DNA fragmentation and cell death in HL-60 human promyelocytic leukemia cells by pharmacological inhibitors of protein kinase C. *Cancer Res* 1994;54:1707–14.
22. Essassi D, Zini R, Tillement JP. Use of 1-anilino-8-naphthalene sulfonate as a fluorescent probe in the investigation of drug interactions with human alpha-1-acid glycoprotein and serum albumin. *J Pharm Sci* 1990;79:9–13.
23. Imamura H, Maruyama T, Otagiri M. Evaluation of quinaldine red as a fluorescent probe for studies of drug-alpha 1-acid glycoprotein interaction. *Biol Pharm Bull* 1993;16:926–9.
24. Block T, Petrides G, Kushner H, Kalin N, Belanoff J, Schatzberg A. Mifepristone plasma level and glucocorticoid receptor antagonism associated with response in patients with psychotic depression. *J Clin Psychopharmacol* 2017;37:505–11.
25. Block TS, Kushner H, Kalin N, Nelson C, Belanoff J, Schatzberg A. Combined analysis of mifepristone for psychotic depression: plasma levels associated with clinical response. *Biol Psychiatry* 2018;84:46–54.
26. Swahn ML, Wang G, Aedo AR, Cekan SZ, Bygdeman M. Plasma levels of antiprogesterin RU 486 following oral administration to non-pregnant and early pregnant women. *Contraception* 1986;34:469–81.
27. Liu JH, Garzo VG, Yen SS. Pharmacodynamics of the antiprogesterone RU486 in women after oral administration. *Fertil Steril* 1988;50:245–9.
28. de Vries B, Walter SJ, Wolfs TG, Hocheppied T, Rabina J, Heeringa P, et al. Exogenous alpha-1-acid glycoprotein protects against renal ischemia-reperfusion injury by inhibition of inflammation and apoptosis. *Transplantation* 2004;78:1116–24.
29. Levis M, Tse KF, Smith BD, Garrett E, Small D. A FLT3 tyrosine kinase inhibitor is selectively cytotoxic to acute myeloid leukemia blasts harboring FLT3 internal tandem duplication mutations. *Blood* 2001;98:885–7.
30. Nguyen B, Williams AB, Young DJ, Ma H, Li L, Levis M, et al. FLT3 activating mutations display differential sensitivity to multiple tyrosine kinase inhibitors. *Oncotarget* 2017;8:10931–44.
31. Knapper S, Burnett AK, Littlewood T, Kell WJ, Agrawal S, Chopra R, et al. A phase 2 trial of the FLT3 inhibitor lestaurtinib (CEP701) as first-line treatment for older patients with acute myeloid leukemia not considered fit for intensive chemotherapy. *Blood* 2006;108:3262–70.
32. Levis M, Allebach J, Tse KF, Zheng R, Baldwin BR, Smith BD, et al. A FLT3-targeted tyrosine kinase inhibitor is cytotoxic to leukemia cells in vitro and in vivo. *Blood* 2002;99:3885–91.
33. Smith BD, Levis M, Beran M, Giles F, Kantarjian H, Berg K, et al. Single-agent CEP-701, a novel FLT3 inhibitor, shows biologic and clinical activity in patients with relapsed or refractory acute myeloid leukemia. *Blood* 2004;103:3669–76.
34. Stone RM, Mandrekar SJ, Sanford BL, Laumann K, Geyer S, Bloomfield CD, et al. Midostaurin plus chemotherapy for acute myeloid leukemia with a FLT3 mutation. *N Engl J Med* 2017;377:454–64.
35. Thiede C, Steudel C, Mohr B, Schaich M, Schakel U, Platzbecker U, et al. Analysis of FLT3-activating mutations in 979 patients with acute myelogenous leukemia: association with FAB subtypes and identification of subgroups with poor prognosis. *Blood* 2002;99:4326–35.
36. Boissel N, Cayuela JM, Preudhomme C, Thomas X, Gardel N, Fund X, et al. Prognostic significance of FLT3 internal tandem repeat in patients with de novo acute myeloid leukemia treated with reinforced courses of chemotherapy. *Leukemia* 2002;16:1699–704.
37. Frohling S, Schlenk RF, Breitruck J, Benner A, Kreitmeier S, Tobis K, et al. Prognostic significance of activating FLT3 mutations in younger adults (16 to 60 years) with acute myeloid leukemia and normal cytogenetics: a study of the AML Study Group Ulm. *Blood* 2002;100:4372–80.
38. Moreno I, Martin G, Bolufer P, Barragan E, Rueda E, Roman J, et al. Incidence and prognostic value of FLT3 internal tandem duplication and D835 mutations in acute myeloid leukemia. *Haematologica* 2003;88:19–24.
39. Schmalbrock LK, Cocciardi S, Dolnik A, Agrawal M, Theis F, Jahn N, et al. Clonal evolution of FLT3-ITD positive AML in patients treated with midostaurin in combination with chemotherapy within the ratify (CALGB 10603) and AMLSG 16-10 trials. *Blood* 2017;130:182.
40. Manley PW, Caravatti G, Furet P, Roesel J, Tran P, Wagner T, et al. Comparison of the kinase profile of midostaurin (Rydapt) with that of its predominant metabolites and the potential relevance of some newly identified targets to leukemia therapy. *Biochemistry* 2018;57:5576–90.
41. Zarrinkar PP, Gunawardane RN, Cramer MD, Gardner MF, Brigham D, Belli B, et al. AC220 is a uniquely potent and selective inhibitor of FLT3 for the treatment of acute myeloid leukemia (AML). *Blood* 2009;114:2984–92.
42. Sausville EA, Lush RD, Headlee D, Smith AC, Figg WD, Arbus SG, et al. Clinical pharmacology of UCN-01: initial observations and comparison to preclinical models. *Cancer Chemother Pharmacol* 1998;42:S54–9.
43. Katsuki M, Chuang VT, Nishi K, Kawahara K, Nakayama H, Yamaotsu N, et al. Use of photoaffinity labeling and site-directed mutagenesis for identification of the key residue responsible for extraordinarily high affinity binding of UCN-01 in human alpha-1-acid glycoprotein. *J Biol Chem* 2005;280:1384–91.
44. Kurata N, Matsushita S, Nishi K, Watanabe HH, Kobayashi S, Suenaga A, et al. Characterization of a binding site of UCN-01, a novel anticancer drug on alpha-acid glycoprotein. *Biol Pharm Bull* 2000;23:893–5.

45. Tinguely D, Baumann P, Conti M, Jonzier-Perey M, Schopf J. Inter-individual differences in the binding of antidepressives to plasma proteins: the role of the variants of alpha 1-acid glycoprotein. *Eur J Clin Pharmacol* 1985;27:661-6.
46. Huang JX, Cooper MA, Baker MA, Azad MA, Nation RL, Li J, et al. Drug-binding energetics of human alpha-1-acid glycoprotein assessed by isothermal titration calorimetry and molecular docking simulations. *J Mol Recognit* 2012;25:642-56.
47. Fuse E, Kuwabara T, Sparreboom A, Sausville EA, Figg WD. Review of UCN-01 development: a lesson in the importance of clinical pharmacology. *J Clin Pharmacol* 2005;45:394-403.
48. Sausville EA. Dragons 'round the fleece again: STI571 versus alpha1 acid glycoprotein. *J Natl Cancer Inst* 2000;92:1626-7.
49. Zeitlinger MA, Derendorf H, Mouton JW, Cars O, Craig WA, Andes D, et al. Protein binding: do we ever learn? *Antimicrob Agents Chemother* 2011;55:3067-74.
50. Dente L, Ruther U, Tripodi M, Wagner EF, Cortese R. Expression of human alpha 1-acid glycoprotein genes in cultured cells and in transgenic mice. *Genes Dev* 1988;2:259-66.
51. Dewey MJ, Rheaume C, Berger FG, Baumann H. Inducible and tissue-specific expression of rat alpha-1-acid glycoprotein in transgenic mice. *J Immunol* 1990;144:4392-8.
52. Williams AB, Nguyen B, Li L, Brown P, Levis M, Leahy D, et al. Mutations of FLT3/ITD confer resistance to multiple tyrosine kinase inhibitors. *Leukemia* 2013;27:48-55.